European Journal of Medicinal Chemistry 89 (2015) 179–188

Contents lists available at ScienceDirect

European Journal of Medicinal Chemistry

journal homepage: http://www.elsevier.com/locate/ejmech

Original article

Identification and nanoentrapment of polyphenolic phytocomplex from *Fraxinus angustifolia*: *In vitro* and *in vivo* wound healing potential

Kenza Moulaoui [a], Carla Caddeo [b], Maria Letizia Manca [b], Ines Castangia [b], Donatella Valenti [b], Elvira Escribano [c], Djebbar Atmani [a], Anna Maria Fadda [b], Maria Manconi [b, *]

[a] Laboratory of Applied Biochemistry, Faculty of Life and Nature Science, University of Bejaia, Algeria
[b] Dept. Scienze della Vita e dell'Ambiente, University of Cagliari, Italy
[c] Biopharmaceutics and Pharmacokinetics Unit, Institute for Nanoscience and Nanotechnology, University of Barcelona, Spain

ARTICLE INFO

Article history:
Received 4 July 2014
Received in revised form
1 October 2014
Accepted 15 October 2014
Available online 16 October 2014

Keywords:
Vesicle
Fraxinus angustifolia
Polyphenol extract
Oxidative stress
Wound healing

ABSTRACT

The aim of the present study was to elucidate the polyphenolic composition of *Fraxinus angustifolia* leaf and bark extracts, and to evaluate their efficacy in wound healing. Quercetin, catechin, rutin and tannic acid were identified as the main components of the extracts. In order to improve their skin bioavailability, the polyphenolic phytocomplexes were incorporated in different nanovesicles, namely ethosomes and phospholipid vesicles containing Transcutol® P (Trc) or ethylene glycol (EG). The latter had never been used before as a component of phospholipid vesicles, and it was found to play a key role in improving extract efficacy in wound healing. Results of cryogenic transmission electron microscopy (cryo-TEM), Photon Correlation Spectroscopy (PCS) and Small-Angle X-ray Scattering (SAXS) showed that ethosomes and EG-PEVs were small, monodispersed, unilamellar vesicles, while Trc-PEVs were larger, less homogeneously dispersed and multilamellar, with a large bilayer thickness. Free extracts did not show relevant ability to protect *in vitro* human keratinocytes from H_2O_2 damages, while when entrapped in nanovesicles, they significantly inhibited H_2O_2 stress damages, probably related to a higher level of cell uptake. On the other hand, *in vivo* results showed that the highest antioxidant and anti-inflammatory effects were provided by the phytocomplexes in EG-PEVs, which favoured wound healing. Moreover, non-entrapped *F. angustifolia* extracts showed a marginal effect, comparable to that of free quercetin dispersion (control).

In conclusion, our results depict that these extracts may find potential applications in biomedicine.

1. Introduction

Fraxinus angustifolia has been extensively used in folk medicine of Algeria as anti-inflammatory and antioxidant, but also as diuretic, digestive and astringent. Recently, the antioxidant capacity of bark extract of *F. angustifolia* and other Algerian plants was measured, and it was attributed to the presence of high amounts of polyphenolic compounds [1,2]. They are plant secondary metabolites, naturally present in fruit and vegetables and, depending on their structure, ranging from simple moieties containing a single hydroxylated aromatic ring, to highly complex polymeric substances, they can be classified into non-flavonoid and flavonoid compounds [3]. Over the past years, great attention has been given to plant polyphenols as efficient free radical scavengers that can actively transfer electrons to endogenous free radicals naturally present in human body. Several physiological and biochemical processes may produce oxygen-centered free radicals and other reactive oxygen species as byproducts. A low amount of radicals can provide helpful bioactivity as signal transducers and growth regulators, but their overproduction may be harmful due to their ability to attack numerous biomolecules (e.g., lipids, proteins, DNA), thus causing oxidative damage and degenerative pathologies [4]. A long and continuous exposure to free radicals may result in an alteration of basal physiological conditions and the development of chronic inflammation, possibly leading to degenerative diseases, such as atherosclerosis, coronary heart problems, ageing and cancer. Several studies have revealed that all natural antioxidants,

* Corresponding author. Dept. Scienze della Vita e dell'Ambiente, University of Cagliari, Via Ospedale 72, 09124 Cagliari, Italy.
E-mail address: manconi@unica.it (M. Manconi).

http://dx.doi.org/10.1016/j.ejmech.2014.10.047
0223-5234/

especially polyphenols, are able to suppress chronic inflammation and prevent or delay various severe diseases, including cancer, thus playing an important role in the prevention and protection of human tissues from oxidative stress [5–7].

Polyphenolic compounds are commonly extracted from native vegetable tissues with organic solvents, among which ethanol is the safest and most biocompatible [8]. Plant extracts may contain other molecules, such as derivatives of tannic acid, terpens and anthocyanins, which can exert a complementary activity in the phytocomplex efficacy. The higher efficacy of natural phytocomplexes, with respect to single drugs, is well known in phytotherapy [9]. The association of several natural compounds isolated from traditional medicinal plants may serve as novel therapeutic complexes where different molecules can act synergically. The major limitation to effective therapeutic application of these phytocomplexes is due to their low *in vivo* bioavailability, especially when they are applied on the skin. Recent studies demonstrated the improvement of the therapeutic efficacy of different natural compounds by the nanoencapsulation in lamellar vesicles [10–14]. Such carriers mostly improved drug penetration and accumulation in intact skin, acting as penetration enhancers or as carriers [11,14–16]. When those vesicles were applied on damaged skin, they enhanced drug local bioavailability by avoiding formulation leakage, increasing the drug residence time in damaged tissues and facilitating drug internalization into the cells. In this way, liposome-like vesicles allowed a remarkable enhancement of the anti-inflammatory activity of polyphenols in inhibiting the onset of skin damages induced by phorbol ester (TPA) [17]. Similarly, the efficacy of natural extracts may be improved through their incorporation in lamellar vesicles, thanks to their versatility to load and protect unstable/photosensitive molecules having different structure and molecular weight, and their ability to facilitate and control the delivery of the loaded drug to the target site [18–21].

In this study, the active components of leaves and bark of *F. angustifolia* were extracted using ethanol, and their content in polyphenols was assessed by HPLC. To improve the antioxidant, anti-inflammatory and epithelizing efficacy of the polyphenolic phytocomplexes by increasing their local bioavailability, they were incorporated in liposome-like vesicles containing penetration enhancers (ethanol, Transcutol® P or ethylene glycol), namely ethosomes, Trc-PEVs and EG-PEVs. The vesicles were characterized by structure, morphology, size and zeta potential. The ability of free and nanoentrapped polyphenolic phytocomplexes to scavenge DPPH and ABTS free radicals, chelate ferrous ion, and protect human keratinocytes against hydrogen peroxide-induced oxidative stress were evaluated. Further, their efficacy as antioxidant and anti-inflammatory products was evaluated in a mouse model of skin lesion induced by phorbol ester (TPA) and compared to that of pure quercetin, one the most potent natural antioxidant and anti-inflammatory agent.

2. Experimental section

2.1. Materials

Phospholipon®50 (P50), a mixture of soybean phospholipids containing 45% of phosphatidylcholine and 10–18% of phosphatidylethanolamine, triglycerides and fatty acids, was a gift from AVG S.r.l. (Milan, Italy) and Lipoid GmbH (Ludwigshafen, Germany). Diethylene glycol monoethyl ether (Transcutol® P, Trc) was donated by Gattefossè (Saint Priest, France). Ethanol, ethylene glycol (EG), 12-O-Tetradecanoylphorbol 13-acetate (TPA) and all other reagents were purchased from Sigma–Aldrich (Milan, Italy).

2.2. Plant extraction and identification of main components

Fresh leaves and bark of *F. angustifolia* were collected early summer from a remote area in the forest of Azrun Bechar, Province of Amizour, Northeastern Algeria. The plant was identified in the laboratory of Botany, University of Bejaia, Algeria. Both parts of plant were air-dried, ground to fine powder (63 μm diameter) and separately extracted in ethanol (1:4 w/v) under continuous stirring at room temperature for 24 h. After centrifugation (1500× *g*), extracts were evaporated and stored at −20 °C until use. Dry extracts of *F. angustifolia* leaves and bark were used for all experiments.

The components of both extracts were separated by high performance liquid chromatography (HPLC) using a chromatograph Alliance 2690 (Waters, Milan, Italy) equipped with a photodiode array detector and a computer integrating apparatus (Empower™ 3). The column was a DiscoveryBio C5 (5 μm, 4.6 × 300 mm, Supelco). The mobile phase was a mixture of methanol, water, acetonitrile and acetic acid (40:41.94:18:0.06, v/v), delivered at a flow rate of 0.3 ml/min. The identification of the major components was carried out using reference standards.

2.3. Vesicle preparation

Each extract was dispersed (5 mg/ml) in a mixture of ethanol/water, ethylene glycol/water or Transcutol/water (1:1, v/v), then P50 (60 mg/ml) was added and left hydrating overnight. The suspensions were sonicated (2 s on and 2 s off, 50 cycles; 13 μm of probe amplitude) with a high intensity ultrasonic disintegrator (Soniprep 150, MSE Crowley, London, United Kingdom). Empty vesicles were also prepared and used as a reference.

Samples were purified from the non-incorporated drug by dialysis using dialysis tubing (Spectra/Por® membranes: 12–14 kDa MW cut-off, 3 nm pore size; Spectrum Laboratories Inc., DG Breda, The Netherlands).

2.4. Vesicle characterization

Vesicle formation and morphology were checked by cryogenic transmission electron microscopy (cryo-TEM). A thin aqueous film was formed by placing a sample drop on a glow-discharged holey carbon grid and then blotting the grid against filter paper. The film was vitrified by plunging the grid in ethane maintained at its melting point with liquid nitrogen, using a Vitrobot (FEI Company, Eindhoven, The Netherlands). The vitreous films were transferred to a Tecnai F20 TEM (FEI Company) and the samples were observed in a low-dose mode. Images were acquired at 200 kV at a temperature between −170–175 °C, using low-dose imaging conditions not exceeding 20 $e^{-}/Å^{2}$, with a CCD Eagle camera (FEI Company).

The average diameter and polydispersity index (PI; a measure of the size distribution width) were determined by Photon Correlation Spectroscopy (PCS) using a Zetasizer nano-ZS (Malvern Instruments, Worcestershire, United Kingdom). Samples were backscattered by a helium–neon laser (633 nm) at an angle of 173° and a constant temperature of 25 °C. Zeta potential was estimated using the Zetasizer nano-ZS by means of the M3-PALS (Mixed Mode Measurement-Phase Analysis Light Scattering) technique, which measures the particle electrophoretic mobility.

Entrapment Efficiency (EE%), expressed as the percentage of extract actually entrapped into the vesicles (post-dialysis) versus the amount initially used (pre-dialysis), was determined by HPLC after disruption of vesicles with methanol (1:1000). Analyses were performed working at four different wavelengths (i.e., 210, 233, 410 and 440 nm) corresponding to the main components identified (i.e., rutin, catechin, tannic acid and quercetin) and using

calibration curves of the standards (ABS against concentration) to quantify the extract components. Results were expressed as the mean of the values obtained at the above reported wavelengths.

The lipid content of dispersions was determined by the Stewart method [22]. An aliquot of suspension was added to a biphasic mixture of aqueous ammonium ferrithiocyanate solution (0.1 N) and chloroform. The concentration of P50 was obtained by measuring the absorbance at 485 nm in the organic solution. The aggregation efficiency (AE%) represented the effective amount of aggregated phospholipids expressed as the percentage of the amount initially used.

2.5. Small-Angle X-ray Scattering (SAXS) of vesicles

SAXS studies were carried out using a S3-MICRO (Hecus X-ray systems, Graz, Austria). Cu Kα ($\lambda = 1.542$ Å) radiation was provided by a fine-focus Cu anode source. The working q-range was 0.003–0.6 $Å^{-1}$, where $q = (4\pi \sin\theta)/\lambda$ is the modulus of the scattering wave vector, θ the scattering angle and λ the wavelength. All scattering curves, recorded at 25 °C, were reproduced three times and a representative curve was selected, plotting the scattering intensity (I) as a function of the scattering vector (q). SAXS patterns were analysed in terms of a global model using the program GAP (Global Analysis Program) developed by Pabst [23], which permitted to obtain relevant structural parameters on bilayer-based structures, i.e. vesicles and lamellar phases. From the analysis, the membrane thickness was obtained through the definition $d_B = 2(z_H + 2\sigma_H)$. z_H and σ_H derive from SAXS curve fitting with GAP.

2.6. Antioxidant activity assay

2.6.1. DPPH radical scavenging assay

The antioxidant activity of ethanolic solutions of leaf and bark extracts, empty vesicles and leaf or bark extract-loaded vesicles was tested measuring their ability to scavenge 2,2-diphenyl-1-picrylhydrazyl (DPPH). Each sample was added (1:50) to DPPH methanolic solution (25 μM). All samples were stored at room temperature for 30 min, in the dark. Then, the absorbance was measured at 517 nm against blank. All the experiments were performed in triplicate. The percent antioxidant activity (or free radical scavenging activity) was calculated according to the following formula [24]: antioxidant activity (%) = $[(ABS_{DPPH} - ABS_{sample})/ABS_{DPPH}] \times 100$.

2.6.2. ABTS radical cation decolorization assay

ABTS (2,2-azinobis (3-ethylbenzothiazoline-6-sulfonic acid) diammonium salt; 7 mM) is converted to coloured radical cation $ABTS^{\bullet+}$ by oxidation with potassium persulfate (2.45 mM), after incubation in the dark at room temperature for 12–16 h [25]. Test samples were diluted in methanol (100 μg/ml) and added to reactive solution, whose decolorization was monitored by absorption decrease at 734 nm. All the experiments were performed in triplicate. The percent of antioxidant activity was calculated according to the formula: antioxidant activity (%) = $[(ABS_0 - ABS)/ABS_0] \times 100$, where ABS_0 and ABS represent the absorbance of the control and the sample, respectively.

2.7. Metal ion-chelating assay

The ferrous ion-chelating potential of the extract was investigated by measuring the ability of samples to chelate Fe^{2+} by monitoring the ferrous iron-ferrozine complex formation at 562 nm [26] Briefly, 500 μl of each sample (100 μg/ml) was added to 100 μl of $FeCl_2$ (0.6 mM), 500 μl of methanol and 200 μl of ferrozine (5 mM), vigorously shaken and incubated for 10 min at room temperature. All the experiments were performed in triplicate. The percent of chelating activity was expressed according to the following equation: Chelation Activity (%) = $[(ABS_0 - ABS)/ABS_0] \times 100$, where ABS_0 and ABS are the absorbance of the control and the sample, respectively.

2.8. Cell viability studies (MTT assay)

Human keratinocytes were used at passages 2–4. Cells were grown as monolayer in 35 mm tissue culture dishes incubated at 37 °C in humidified atmosphere of 5% CO_2 in air. Iscove's Modified

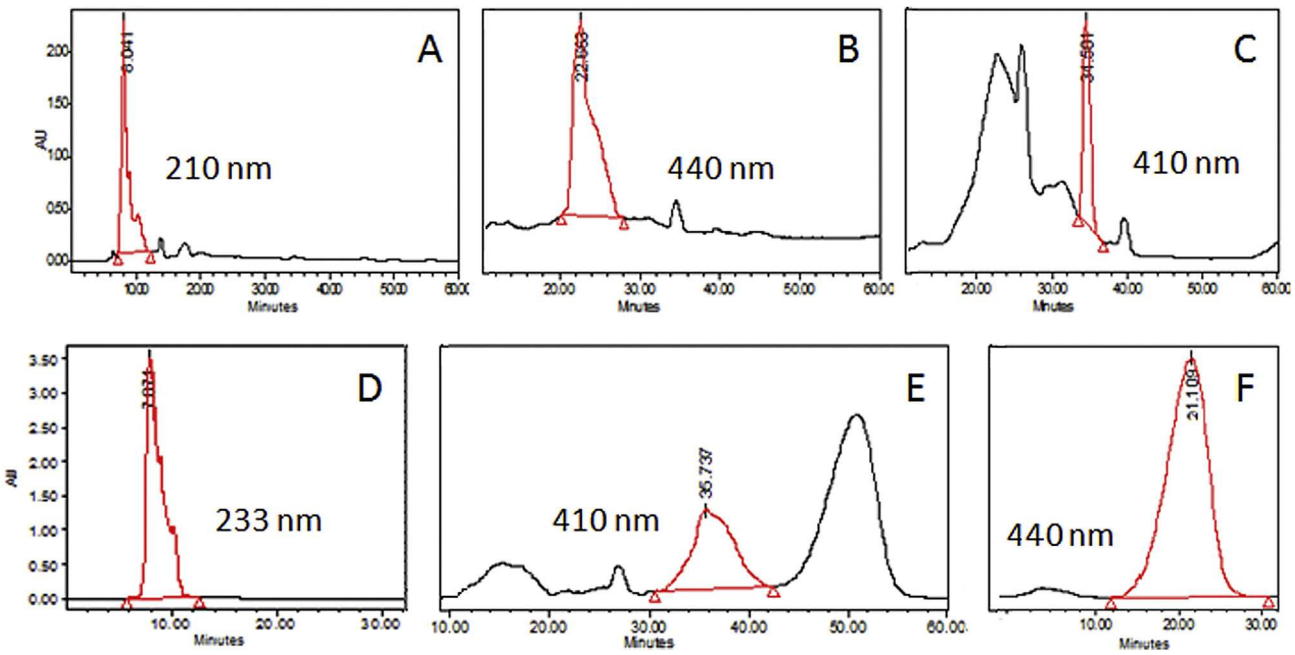

Fig. 1. Chromatograms at different wavelengths of identified components of leaf extract: rutin (A), quercetin (B) and tannic acid (C); and components of bark extract: catechin (D), tannic acid (E) and quercetin (F).

Dulbecco's Medium, containing L-glutamine, supplemented with 20% foetal bovine serum (FBS), 10% penicillin/streptomycin and 10% fungizone, was used as growth medium. Cells were seeded into 96-well plates at a density of 7.5×10^3 cells/well. After 24 h of incubation, cells were treated for 2, 4, 24 and 48 h with leaf and bark extract solution and extract-loaded vesicles at different dilutions (1:50, 1:100, 1:1000, 1:10,000). Cell viability was determined by the MTT [3(4,5-dimethylthiazolyl-2)-2, 5-diphenyltetrazolium bromide] colourimetric assay, adding 500 μl of MTT reagent (0.5 mg/ml in PBS) to each well. After 2 h, the formed formazan crystals were dissolved in DMSO and their concentration was spectrophotometrically quantified at 570 nm with a microplate reader (Synergy 4, Reader BioTek Instruments, AHSI S.p.A, Bernareggio, Italy). All experiments were repeated at least three times and in triplicates. Results are shown as percent of cell viability in comparison with non-treated control cells (100% viability).

2.9. Antioxidant activity of samples against oxidative stress in human keratinocytes

Cells were seeded into 24-well plates at a density of 5×10^4 cells/well. After 24 h of incubation, cells were treated for 4 h with hydrogen peroxide (1:30000) and leaf and bark extract solution or vesicles (final concentration of extracts 0.1 mg/ml). Non-treated cells were used as a control. After 4 h of incubation cell were washed 3 times with fresh medium and cell viability was determined by the MTT as reported above. Final results are reported as the percentage of control cells (100% viability).

2.10. Cell uptake of fluorescent vesicles

The internalization of *F. angustifolia* extracts by keratinocytes was studied by confocal microscopy. For this purpose, vesicles were labelled with a lipophilic fluorescent marker (1,2-dioleolyl-sn-glycero-3-phosphoethanolamine-N-lissamine-sulfo-rhodamineB; Rho-PE 0.035 mg/ml) and loaded with a hydrophilic fluorescent marker (5(6)-carboxyfluorescein; CF 0.025 mg/ml). The keratinocytes were cultured on glass slides and the experiments were performed at sub-confluence. The cells were incubated at 37 °C with the different formulations for 3, 6 and 24 h. Afterwards, the cells were washed, fixed with 4% paraformaldehyde and treated with Triton X-100 (0.1%) to increase the permeability of the cell membrane. The fixed cells were stained with Hoechst 33258 (blue) to visualize cell nucleus.

The images were obtained using a confocal inverted microscope FluoView FV1000 (Olympus, Barcelona, Spain) equipped with an ultraviolet–visible light laser; a 60× objective UPLSAPO was used. RhoPE, CF and Hoechst were visualized with a wavelength of excitation/emission of 559/578 nm, 470/535 nm, 360/460 nm, respectively.

2.11. In vivo oedema and myeloperoxidase assays

Male CD-1 mice (5–6 weeks old, 25–35 g) were obtained from Harlan Laboratories (S. Pietro al Natisone, Udine, Italy) and acclimatized for 1 week before use. All animal experimentations have been conducted in accordance with the guidelines for care and use of experimental animals of the European Communities Council Directive 86/609/EEC.

The back skin of mice ($n = 4$ per group) was shaved 1 day before the experiment, and those animals showing no hair re-growth were used. TPA dissolved in acetone (3 μg/20 μl) was applied to the shaved dorsal area (~2 cm^2) to induce cutaneous inflammation and ulceration (day 1). Negative control mice received acetone only (20 μl). All test samples (20 μl) were topically smeared over the same dorsal site 3 and 6 h after TPA application. The procedure was repeated (at 24-h intervals) on day 2 and 3. On day 4, mice were sacrificed by cervical dislocation. Oedema formation and myeloperoxidase (MPO) activity were measured. The treated dorsal skin area of mice was excised, weighed to assess any increase indicative of oedema formation. MPO assay was performed following the previously reported method [27]. Briefly, skin biopsies were homogenized and centrifuged, the supernatant was incubated with hydrogen peroxide and tetramethylbenzidine, and then assayed for MPO activity spectrophotometrically at 620 nm. The MPO activity was calculated from the linear portion of a standard curve.

2.12. Statistical analysis of data

Results are expressed as the mean ± standard deviation. Analysis of variance (ANOVA) and Scheffe's test for multiple comparisons of means were performed using IBM SPSS statistics for Windows.

3. Results

3.1. Extract and vesicle characterization

Polyphenols (including flavonoids) are the largest and most widespread classes of plant constituents, and their presence in *F. angustifolia* extract was previously confirmed [1]. In the present work, the polyphenols in bark and leaf extracts were identified in HPLC using a photodiode detector, which is crucial to component detection thanks to its capability to simultaneously monitor several wavelengths. However, the main phenolic compounds of *F. angustifolia* were difficult to separate by HPLC, and an acceptable separation was possible only using a 30 cm column and a low flux (0.3 ml/min). The UV spectra of the major peaks in the chromatograms indicated that the compounds were probably not completely pure, and additional neo-interactions were present in both extracts. The most abundant polyphenols identified were quercetin, rutin and tannic acid in leaf extract, catechin, quercetin and tannic acid in bark extract (Fig. 1). The anti-inflammatory and antioxidant activity of these free phenols have been largely probed, and can be limited by their low bioavailability.

Having this in mind, leaf and bark polyphenolic phytocomplexes of *F. angustifolia* were incorporated in ethosomes and PEVs containing a high amount of water cosolvent (50%, v/v). Cryo-TEM micrographs (Fig. 2) showed that all vesicles were spherical, but their lamellarity and size was dependent on the composition of samples, especially on the cosolvent used. Indeed, ethosomes and EG-PEVs appeared basically unilamellar, small in size and highly homogeneously dispersed, while Trc-PEVs were larger, multilamellar and with a larger size distribution. Results were confirmed by PCS measurements (Table 1). Regardless the extract loaded, EG-PEVs were the smallest vesicles (~100 nm), ethosomes were slightly larger (~128 nm), and Trc-PEVs were the largest ones (~200 nm). Ethosomes were particularly monodispersed (PI~0.05), as PI of EG-PEVs and Trc-PEVs was 0.15 and 0.29, respectively. Zeta potential was negative and statistically similar for all the tested formulations, ranging from −41 to −54 mV.

Entrapment efficiency of the 3 main components and aggregation efficiency were comparable for all the formulations: ~40% and ~75%, respectively. Results indicated a satisfactory incorporation of both extracts, as well as a good aggregation of phospholipids, if considering that a high amount of water cosolvent usually favours the drug and phospholipid solubilization, decreasing the entrapment and aggregation efficiency [15].

To evaluate the effect of the cosolvents and extracts on vesicle structure and bilayer parameters, ethosomes and PEVs were

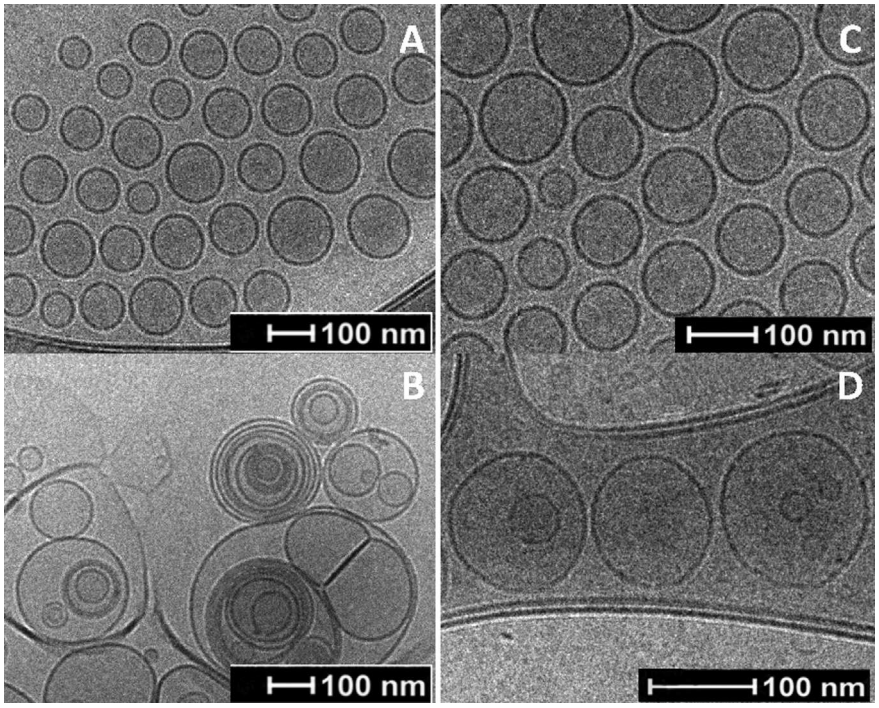

Fig. 2. Cryo-TEM micrographs of leaf extract-loaded ethosomes (A), bark extract-loaded Trc-PEVs (B), bark extract-loaded EG-PEVs (C) and leaf extract-loaded EG-PEVs (D).

analysed by SAXS and compared with empty liposomes. Hypothesised structure and calculated parameters obtained from SAXS for empty and extract-loaded vesicles are reported in Table 2, while representative fitting curves are reported in Fig. 3. Ethosomes and EG-PEVs showed a low-intense, enlarged band characteristic of unilamellar vesicles. Trc-PEVs displayed a sharp and intense peak indicative of multilamellar vesicles. As previously reported for phospholipid vesicles, empty P50 liposomes had a bilayer thickness (d_B) around 49 Å, and a polar head amplitude (σ_H) around 3.2 Å [17]. Some bilayer modifications occurred in empty and leaf or bark extract-loaded vesicles, mostly dependent on the water cosolvent used, while the effect of the extract incorporation was not relevant. Ethosomes and EG-PEVs were as unilamellar as empty liposomes, and their bilayer thickness was only slightly lower (~45 Å) than that of liposomes. In ethosomes, the decrease was a consequence of the reduction of the polar head distance to the centre of bilayer (Z_H), which varied from ~18.1 Å in liposomes to ~15.0 Å, revealing an interdigitated bilayer [28]. Conversely, in EG-PEVs the decrease in bilayer thickness was associated to a more evident reduction in the polar head amplitude (σ_H) around 2 Å. Trc-vesicles were multilamellar, as also observed in cryo-TEM micrographs, and possessed the largest bilayer thickness (~60 Å) due to an increase in both parameters, σ_H and Z_H.

3.2. *In vitro cytotoxicity, cell uptake and antioxidant ability of nanoentrapped extracts*

The cytotoxicity of extract ethanolic solutions and empty or extract loaded vesicles was tested in human keratinocytes, first as a function of sample concentration (Fig. 4A). After 48 h of incubation with all samples, cell toxicity was not dose-dependent but composition-dependent. Indeed, empty vesicle viability ranged between 90% and 105%. Leaf extract solution and vesicles allowed a viability (~90%) comparable to that of empty vesicles and higher than that of samples containing bark extract (~78%), whose incorporation in vesicles did not affect viability. The highest extract concentration tested (P50 1.2 mg/ml and extract 100 μg/ml), causing maximum mortality (~29%), was used for further studies: cytotoxicity tests as a function of time (2, 4, 24 and 48 h) and antioxidant activity. The viability of cells incubated with empty and extract loaded vesicles was >100% up to 24 h, lower when the solutions were used, and decreased after 48 h of incubation (~80%), presumably due to an excessive accumulation of metabolites in the unchanged medium (Fig. 4B).

Vesicles were labelled with a membrane marker (Rho-PE) and hydrophilic carboxy fluorescein (CF) to identify the aqueous compartment, and their internalization by human keratinocytes was checked at 3, 6 and 24 h using a confocal laser microscope (Fig. 5). At each time point, free Rho-PE and CF dispersion adhered to cell surface and was not internalized. Only at 24 h a slight CF fluorescence was detected in the cytoplasm. On the contrary, labelled ethosomes and Trc-PEVs showed a rapid (3 h) internalization of CF, increasing up to 24 h, while Rho-PE remained in the intercellular medium. EG-PEVs were successfully internalized by keratinocytes: after 3 h, only the green fluorescence was evident, while at 24 h both CF and Rho-PE were clearly internalized, demonstrating vesicle uptake into cell cytoplasm.

Usually, the antioxidant activity of plant extracts is associated to their content in polyphenolic compounds: several works report a linear relationship between antioxidant power and polyphenol content [2]. To confirm this, the ability of leaf and bark extracts, in ethanolic solution or entrapped in vesicles, to protect cells against H_2O_2-induced oxidative stress was tested [29]. The viability of H_2O_2-stressed cells treated with leaf and bark solutions was statistically similar to H_2O_2-only receiving cells (~30%, $p > 0.05$), denoting no efficacy of ethanol in facilitating phytocomplex interaction with keratinocytes (Table 3). Conversely, the inclusion of both extracts in vesicles potentiated their antioxidant power, since the viability was higher and reached 80%, presumably because vesicles facilitated extract internalization by cells. Extract-loaded

Table 1
Mean diameter (MD), polydispersity index (PI), zeta potential (ZP), entrapment efficiency (EE) and aggregation efficiency (AE) of leaf and bark extract-loaded vesicles. Mean values ± standard deviation (SD) were obtained from at least 6 samples. $^{○,+,§}$ indicate differences within pairs ($p > 0.05$) and between groups ($p < 0.05$).

Sample	MD (nm)	PI	ZP (mV)	EE (%)	AE (%)
Leaf ethosomes	$^{○}$128 ± 3	0.05	−42 ± 11	40 ± 6	68 ± 8
Leaf Trc-PEVs	$^{+}$215 ± 13	0.17	−46 ± 5	39 ± 6	76 ± 6
Leaf EG-PEVs	§95 ± 5	0.29	−43 ± 7	44 ± 8	68 ± 9
Bark ethosomes	$^{○}$127 ± 10	0.04	−54 ± 8	37 ± 9	80 ± 9
Bark Trc-PEVs	$^{+}$194 ± 5	0.13	−41 ± 5	34 ± 11	68 ± 4
Bark EG-PEVs	§105 ± 9	0.29	−48 ± 2	35 ± 8	74 ± 5

Table 2
Polar head amplitude (σ_H), polar head distance to the centre of bilayer (Z_H) and bilayer thickness (d_B) of empty vesicles and leaf or bark extract-loaded vesicles. Empty liposomes were reported as a reference. Vesicles were unilamellar (ULV) or multilamellar (MLV). Each value corresponds to the mean ± standard deviation (SD) of at least 3 measurements.

Sample	Structure	z_H (Å)	σ_H (Å)	d_B (Å)
Empty liposomes	ULV	18.1 ± 0.6	3.2 ± 0.5	49 ± 3
Empty ethosomes	ULV	14.3 ± 0.2	4.1 ± 0.3	45 ± 2
Empty Trc-PEVs	MLV	21.3 ± 0.2	4.3 ± 0.3	60 ± 2
Empty EG-PEVs	ULV	18.6 ± 0.2	2.0 ± 0.2	45 ± 1
Leaf ethosomes	ULV	13.3 ± 0.5	4.2 ± 0.5	43 ± 3
Leaf Trc-PEVs	MLV	21.1 ± 0.4	4.0 ± 0.7	58 ± 4
Leaf EG-PEVs	ULV	17.9 ± 0.4	2.5 ± 0.3	45 ± 2
Bark ethosomes	ULV	16.1 ± 0.5	3.3 ± 0.8	45 ± 4
Bark Trc-PEVs	MLV	21.1 ± 0.2	5.3 ± 0.3	63 ± 2
Bark EG-PEVs	ULV	18.6 ± 0.2	2.1 ± 0.2	45 ± 1

ethosomes were particularly effective in inhibiting almost completely H_2O_2 damages, with respect to the corresponding ethanolic solutions (Table 3).

Additionally, the ability of the formulations to scavenge free radical was assessed by DPPH and ABTS test (Table 4) and to chelate ferrous ion. In DPPH assay, bark extract solution showed a higher antioxidant power (~83%) than leaf extract solution (~74%), and their entrapment in vesicles did not affect the results while in ABTS scavenging the ability of samples (bark and leaves, solution and vesicles) was always similar (~86%). Important differences was observed among extract solution and extract loaded vesicles (ethosomes and PEVs) in ferrous ion-chelating activity in fact the extract incorporation in vesicles allowed an increase of their chelating ability from ~27% (solution) up to ~80%.

3.3. *In vivo antioxidant and anti-inflammatory properties of nanoentrapped extracts*

As reported in a previous work, repeated TPA applications on mouse dorsal skin simulated a model of chronic lesion, and oedema and MPO measurements can be used as indicators of tissue damage and inflammation [17]. The protective effect of *F. angustifolia* polyphenol complexes against TPA damage and the advantage of their nanoencapsulation in vesicles were investigated. Leaf and bark extract ethanolic solutions and a dispersion of quercetin, one of the most abundant and potent natural antioxidant and anti-inflammatory agents, were used as references. Extract solutions and quercetin dispersion were unable to reduce oedema, with respect to TPA-only treated mice (control, $p > 0.05$), even though bark solution led to a significant decrease in MPO activity ($p < 0.05$) (Fig. 6). Among the different extract-loaded vesicles tested, only leaf-loaded EG-PEVs significantly reduced both the parameters (i.e., oedema and MPO activity; $p < 0.01$) leading to basal values of healthy mice. Bark-loaded ethosomes and leaf-loaded Trc-PEVs allowed a reduction in MPO activity ($p < 0.05$), without a statistically significant decrease in oedema. By visual observation, the back of TPA-only treated mice (control) appeared damaged, the skin lost its integrity and an evident and extended wound was present. The treatment with the extracts (either in solution or in vesicles) always reduced tissue loss, resulting in an amelioration of the skin lesion in comparison with the control. The skin treated with leaf samples was always less damaged than that treated with the corresponding bark samples, and the skin treated with the extract loaded vesicles was less damaged than that treated with the corresponding ethanolic solutions. In particular, the skin treated with leaf-loaded EG-PEVs, appeared without injuries or scabs, similarly to healthy mice (Fig. 7).

4. Discussion

In previous works we thoroughly investigated the potential ability of liposome-like systems to promote the antioxidant/anti-inflammatory activity of natural compounds, such as quercetin, curcumin and resveratrol [13,17,30]. In this work, we evaluate the composition and activity of *F. angustifolia* phenolic extracts and present their therapeutic potential against oxidative damage when delivered by the above nanocarriers. Extracts rich in polyphenols can provide additional benefits over the individual components in inhibiting oxidative stress, and an optimized vesicle formulation may further potentiate the effect of the extracts because vesicles are able to avoid the leakage of actives at the application site, improve their accumulation in the target tissues and facilitate cell internalization [14,15]. To achieve high intraliposomal extract concentration, the various components of the phytocomplex will distribute in the different compartments of vesicles, as a function of their lipophilicity/hydrophilicity. In order to facilitate the component solubilization in the water compartments of phospholipid vesicles, a high amount of water cosolvent was necessary (50%, v/v), otherwise liposomes were large (>1000 nm) and polydispersed. A

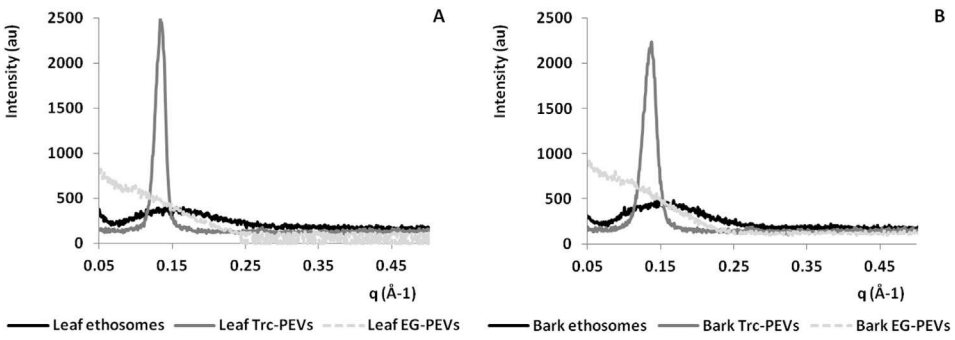

Fig. 3. Representative SAXS diffraction curves as a function of the scattering vector modulus (q) of leaf and bark extract-loaded vesicles.

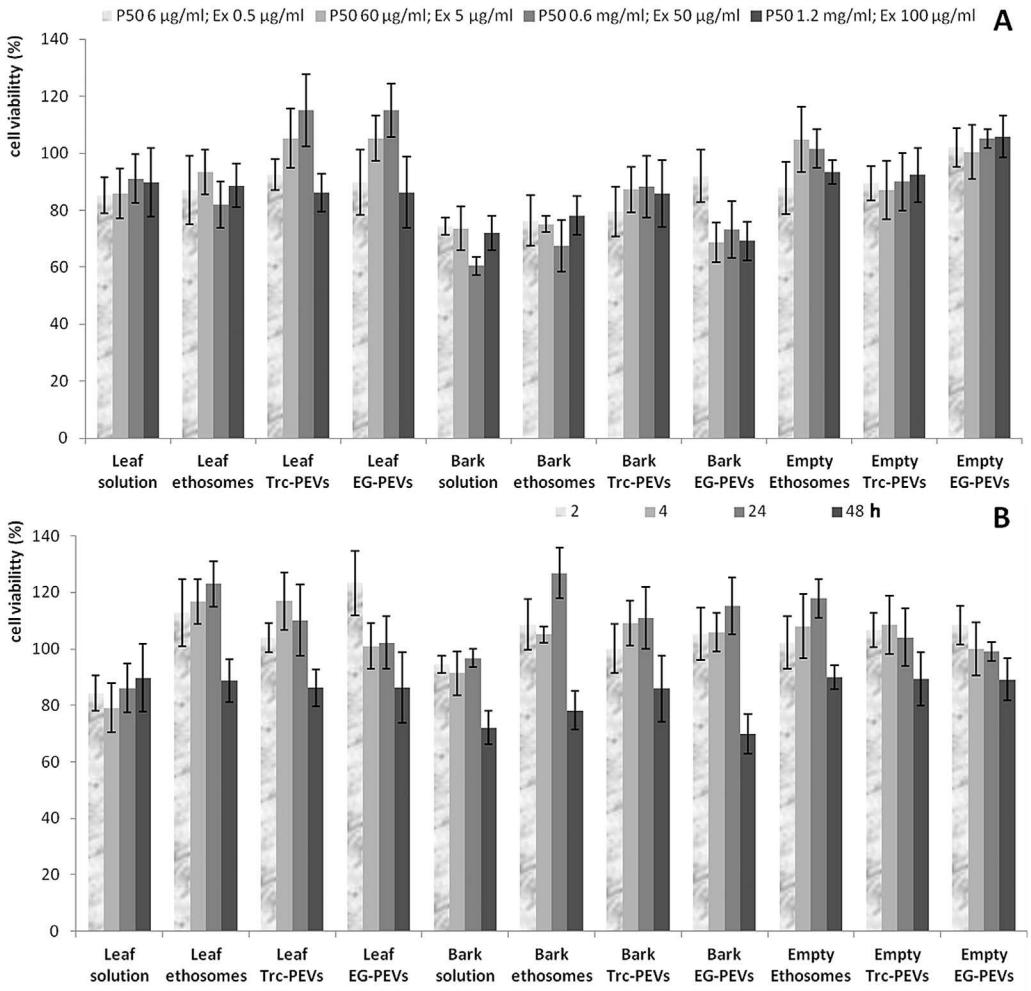

Fig. 4. Viability of human keratinocytes incubated for 48 h with empty vesicles and different concentrations of extract solution or extract-loaded vesicles (A), and for 2, 4, 24 and 48 h with empty vesicles and the solutions/vesicles at the highest extract concentration (100 µg/ml) (B).

preformulation study was carried out using different water cosolvents, and among the obtained formulations, those showing optimal features were selected: ethosomes, Trc-PEVs and EG-PEVs. Ethosomes and EG-PEVs proved particularly promising: they were small (~100 nm), monodispersed (PI < 0.2), with highly negative zeta potential (~−45 mV) that can ensure a long stability of the dispersion [31], and the high cosolvent content (50%, v/v) did not affect the entrapment and aggregation efficiency. Due to their chemical structure, the three cosolvents differently interacted with the vesicle bilayer, leading to peculiar structural modifications. Ethosomes were as unilamellar as conventional liposomes, and according to previous results, ethanol seemed to form an interdigitated bilayer, as it intercalates between the polar heads and enlarges them, forming free spaces between the acyl chains and causing a reduction in the distance between head group and centre of the bilayer (Z_H). Ethylene glycol formed small, unilamellar vesicles with bilayer thickness (d_B) similar to that of ethosomes, but it was not interdigitated because the d_B reduction was due to a contraction of σ_H, indicating a simple interaction of ethylene glycol with the polar heads on vesicle surface. On the contrary, Transcutol intercalated into the lipid acyl chains, as apparent from the formation of multilamellar vesicles having an enlarged bilayer due to the simultaneous increase in both polar head amplitude (σ_H) and Z_H.

Considering that water cosolvents were used at high concentration (50%, v/v), they represent the main component of vesicle dispersion, along with water, and were able to strongly modify vesicle assembly and structure, as well as the distribution of the extract components into the vesicle itself. The structural changes observed in vesicles reflect the different chemical structure of the cosolvents used. They all are alcohols: ethylene glycol is a derivative of ethanol (it posses one more hydroxyl group), Transcutol is a derivative of ethylene glycol (it is diethylene glycol monoethyl ether), thus being larger molecules. These differences between the cosolvents can entail a different localization of the extract components within the vesicles, meaning that each extract loaded in each formulation represents a new carrier system with peculiar characteristics and abilities that can uniquely influence the final delivery of the extracts to the cells and tissue.

Both polyphenolic extracts in ethanolic solution exhibited significant antioxidant activity in the DPPH and ABTS assays, presumably due to quercetin and tannic acid representing the major components of the extracts. Furthermore, their inclusion in the tested vesicles did not affect their antioxidant power. On the contrary, the extract incorporation in vesicles increased their ability to chelate ferrous ions, which are able to generate free radicals from peroxides by Fenton reaction, and induce the production of oxy-radicals and lipid peroxidation. The higher chelating ability of extract-loaded vesicles with respect to extract solutions may be responsible for their superior protective effect against H_2O_2-induced oxidative stress in human keratinocytes, where the

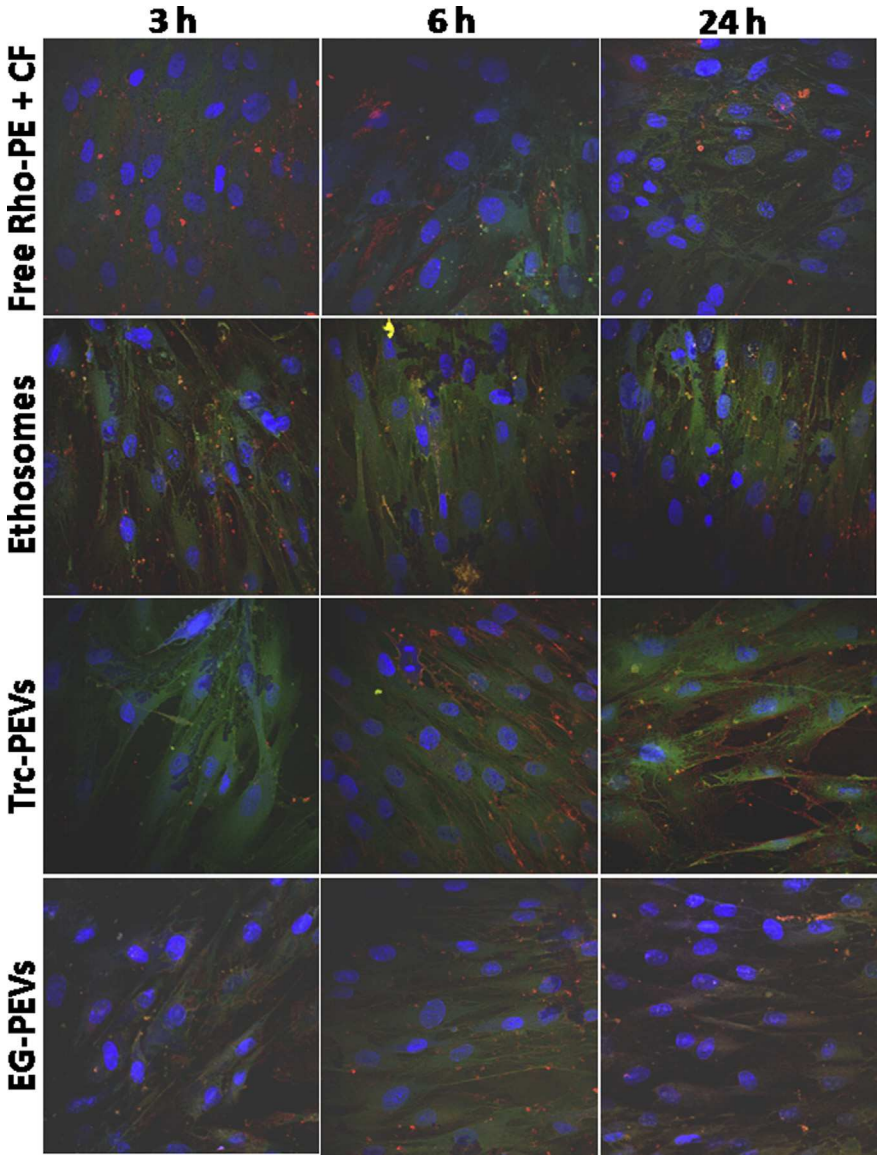

Fig. 5. Confocal laser scanning microscopy images of human keratinocytes incubated for 3, 6 and 24 h with Carboxy Fluorescein (CF)/Rhodamine-PhosphoEthanolamine (Rho-PE) labelled vesicles. The localization and intensity of the dyes are displayed in red for Rho-PE, in green for CF and in blue for the nucleus.

advantage offered by vesicle incorporation was especially evident. Especially leaf and bark ethosomes and bark Trc-PEVs conferred an additional benefit for cell survival and growth, supposedly related to vesicle ability to facilitate the uptake of the loaded actives by the cells. As reported by several authors, phospholipid vesicles facilitate drug internalization inside cells [14,32,33].

Aiming at screening the efficacy of *F. angustifolia* leaf and bark extract loaded in ethosomes and PEVs, we used a previously tested TPA-model of skin lesion [17]. The daily application of TPA mimics the progressive formation of skin lesions and permits the evaluation of the formulation efficacy in preventing lesion degeneration to wound. Further, TPA triggers the inflammation cascade, which naturally occurs in skin lesions, since it causes oedema, leucocyte infiltration and accumulation of oxygen free radicals.

Antioxidant molecules have a fundamental role in inhibiting free radicals and the correlated skin damages, most of them having also anti-inflammatory properties. As previously found for pure quercetin and curcumin, the administration of simple phenolic dispersion did not improve *in vivo* wound healing in mice, while their incorporation in suitable vesicles successfully enhanced their efficacy [13,17]. Likewise, in this work ethanolic solutions of leaf and bark extracts and quercetin dispersion did not provide satisfactory reduction of oedema and MPO activity, or a skin re-epithelisation, although bark solution allowed a decrease in MPO

Table 3
Protective effect of leaf and bark extract ethanolic solutions and vesicles against H_2O_2-induced oxidative stress in human keratinocytes, evaluated as a function of cell survival. Data are reported as mean values ± standard deviation (SD) of cell viability expressed as the percentage of negative control (100% of viability).$^{*}p < 0.05$,$^{**}p < 0.01$ versus H_2O_2-only receiving cells.

Cell viability (MTT)		
Sample	Leaf extract (%±SD)	Bark extract (%±SD)
H_2O_2	24 ± 4	24 ± 4
H_2O_2 + Solution	30 ± 7	34 ± 6
H_2O_2 + Ethosomes	**76 ± 7	**88 ± 9
H_2O_2 + Trc-PEVs	*39 ± 7	**61 ± 8
H_2O_2 + EG-PEVs	*44 ± 3	*46 ± 8

Table 4
Antioxidant activity (%) measured by DPPH, ABTS radical scavenging and ferrous ion-chelating capacity (FICC) by leaf and bark extract ethanolic solutions and vesicles. Data are reported as mean values ± standard deviation (SD) of three determinations.

		DPPH (%±SD)	ABTS (%±SD)	FICC (%±SD)
Leaf extract	Solution	74 ± 2	86 ± 1	30 ± 2
	Ethosomes	72 ± 2	88 ± 1	76 ± 2
	Trc-PEVs	69 ± 3	86 ± 1	81 ± 2
	EG-PEVs	77 ± 3	86 ± 1	86 ± 3
Bark extract	Solution	83 ± 1	87 ± 1	22 ± 2
	Ethosomes	83 ± 1	87 ± 1	72 ± 3
	Trc-PEVs	82 ± 1	87 ± 1	81 ± 3
	EG-PEVs	84 ± 1	85 ± 2	78 ± 4

activity with respect to control TPA mice. Bark extract incorporation in vesicles did not supply important ameliorations of both biomarkers and skin lesions, except when it was delivered by ethosomes, which provided a significant reduction in MPO activity. Notably, bark extract ethosomes showed the highest ability to protect human keratinocytes against oxidative stress and confirmed this ability *in vivo* reducing the MPO activity without affecting oedema and tissue regeneration and remodelling.

On the contrary, leaf extract loaded in vesicles led to an important reduction of MPO activity and the skin appeared less damaged, showing promising features as topical formulations for treatment of chronic inflammation. The nanoincorporation of leaf extract, in particular using EG-PEVs, played a key function in actively promoting wound healing. Indeed, leaf extract solution possessed a low antioxidant activity *in vitro* and did not inhibit oedema and MPO activity *in vivo*, while its incorporation in ethosomes (without statistic significance) and Trc-PEVs led to an increase of its antioxidant activity *in vitro* and a decrease in MPO activity, and upon incorporation in EG-PEVs the highest inhibition of oedema and MPO activity was achieved, returning to basal values of healthy mice. The visual observation of the mouse skin corroborated these results: the skin treated with leaf extract was always more restored. In particular, leaf extract loaded EG-PEVs, despite not showing the highest ability as protective antioxidant *in vitro*, were effectively internalized by cells, inhibiting MPO activity and oedema and promoting skin re-epithelisation and re-modelling at the same time.

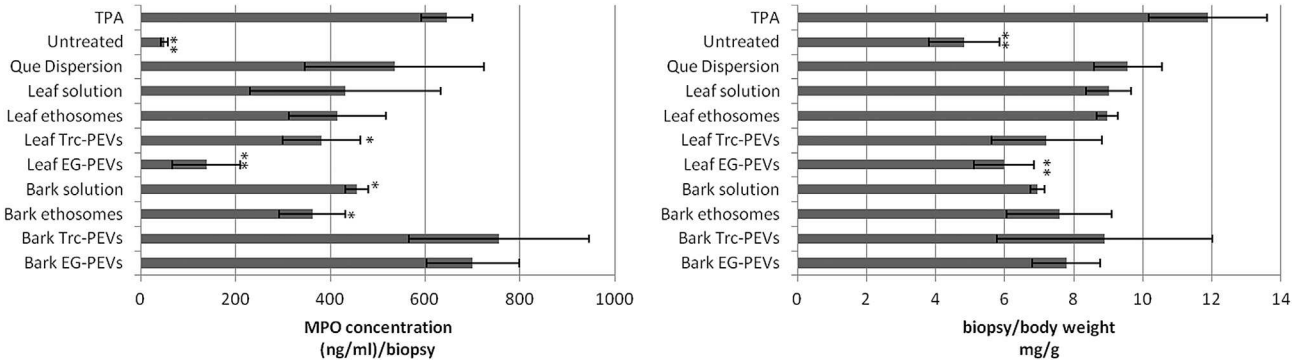

Fig. 6. Mouse oedema and myeloperoxidase (MPO) values ($n = 4$) obtained after TPA treatment followed by application of leaf and bark extract solutions, ethosomes and PEVs or quercetin dispersion used as a reference. Symbols * ($p < 0.05$), ** ($p < 0.01$) indicate statistical differences versus TPA-only treated mouse.

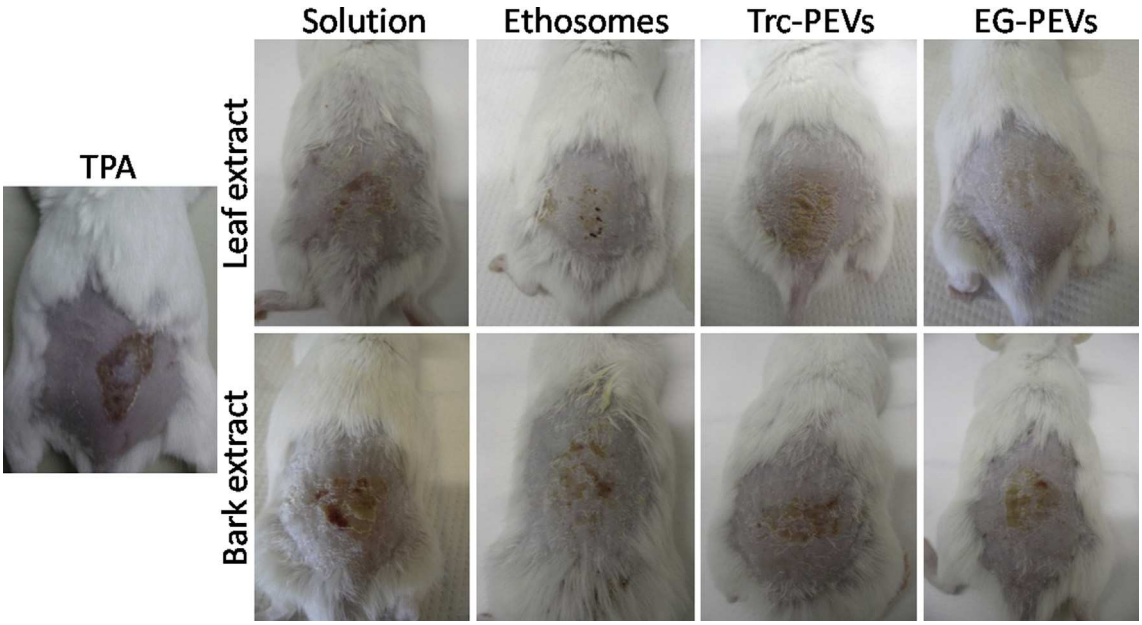

Fig. 7. Photographs of dorsal skin of mice treated with TPA to induce inflammation, and treated with TPA followed by the administration of leaf and bark extract solutions, ethosomes and PEVs.

The results underline that each phytocomplex needs a specific and peculiar carrier to exert its optimal performances *in vivo*, and an ad hoc design is required to formulate new attractive delivery systems.

5. Conclusion

Leaf and bark of *F. angustifolia* contain different antioxidants and anti-inflammatory compounds and their extracts were successfully incorporated in ethosomes and PEVs. The results showed that these vesicles, in particular the new prepared EG-PEVs, were able to improve the leaf phytocomplex local bioavailability, increase the intracellular antioxidant activity in primary human keratinocytes, and consequently promote wound healing in TPA-mouse model with respect to the simple extract ethanolic solution. The important effect of leaf phytocomplex of *F. angustifolia* mediated by PEVs seems to be due both to a direct improvement of extract accumulation in damaged tissue and an efficient antioxidant activity into cells. Hence, EG-PEVs are a promising carrier for natural extract to be used in the pharmaceutical and cosmetic treatment of diseases characterized by free radical oxidative stress and lack of skin integrity, such as photo-damaged skin, skin-ageing, wrinkles and wound healing.

Declaration of interest

The authors report no declarations of interest.

Acknowledgements

This work was supported by a grant from MIUR, Italy (PRIN 2010-2011, Prot. 2010H834LS_004). Dr. C. Caddeo gratefully acknowledges Fondazione Banco di Sardegna for the financial support.

References

[1] D. Atmani, N. Chaher, M. Berboucha, K. Ayouni, H. Lounis, H. Boudaoud, et al., Antioxidant capacity and phenol content of selected Algerian medicinal plants, Food Chem. 112 (2009) 303–309, http://dx.doi.org/10.1016/j.foodchem.2008.05.077.

[2] A. Djeridane, M. Yousfi, B. Nadjemi, D. Boutassouna, P. Stocker, N. Vidal, Antioxidant activity of some algerian medicinal plants extracts containing phenolic compounds, Food Chem. 97 (2006) 654–660, http://dx.doi.org/10.1016/j.foodchem.2005.04.028.

[3] I. Ignat, I. Volf, V.I. Popa, A critical review of methods for characterisation of polyphenolic compounds in fruits and vegetables, Food Chem. 126 (2011) 1821–1835, http://dx.doi.org/10.1016/j.foodchem.2010.12.026.

[4] A. Srinivasan, H.J. Lehmler, L.W. Robertson, G. Ludewig, Production of DNA strand breaks in vitro and reactive oxygen species in vitro and in HL-60 cells by PCB metabolites, Toxicol. Sci. 60 (2001) 92–102. http://www.ncbi.nlm.nih.gov/pubmed/11222876 (accessed 03.09.14.).

[5] F. Menaa, S. Badole, B. Menaa, A. Menaa, S.L. Badhankar, Polyphenols, promising therapeutics for inflammatory diseases?, in: R.R. Watson, V. Preedy (Eds.), Bioact. Food as Diet. Interv. Arthritis Relat. Inflamm. Dis. Bioact. Food Chronic Dis. States, 2012, pp. 421–428.

[6] F. Menaa, A. Menaa, J. Treton, B. Menaa, Nanoencapsulations of Dietary Polyphenols for Oncology and Gerontology: Resveratrol as a Good Example – Resveratrol Nano-formulations: Suitable for Cancer Patients and the Elderly? Introduction to Functional Food Science: Textbook, in: Funct. Food Center/Food Sci. Publ, 2013, pp. 383–404.

[7] F. Menaa, A. Menaa, B. Menaa, Polyphenols nano-formulations for topical delivery and skin tissue engineering, in: R.R. Watson (Ed.), Polyphenols Hum. Heal. Dis, 2014, p. 65.

[8] A. Djeridane, M. Yousfi, B. Nadjemi, N. Vidal, J.F. Lesgards, P. Stocker, Screening of some Algerian medicinal plants for the phenolic compounds and their antioxidant activity, Eur. Food Res. Technol. 224 (2007) 801–809.

[9] M. Kapoor, R. Howard, I. Hall, I. Appleton, Effects of epicatechin gallate on wound healing and scar formation in a full thickness incisional wound healing model in rats, Am. J. Pathol. 165 (2004) 299–307, http://dx.doi.org/10.1016/S0002-9440(10)63297-X.

[10] P.G. Cadena, M.A. Pereira, R.B.S. Cordeiro, I.M.F. Cavalcanti, B. Barros Neto, M. do C.C.B. Pimentel, et al., Nanoencapsulation of quercetin and resveratrol into elastic liposomes, Biochim. Biophys. Acta 1828 (2013) 309–316, http://dx.doi.org/10.1016/j.bbamem.2012.10.022.

[11] L. Tavano, R. Muzzalupo, N. Picci, B. de Cindio, Co-encapsulation of lipophilic antioxidants into niosomal carriers: percutaneous permeation studies for cosmeceutical applications, Colloids Surf. B Biointerfaces 114 (2014) 144–149, http://dx.doi.org/10.1016/j.colsurfb.2013.09.055.

[12] C. Caddeo, K. Teska, C. Sinico, J. Kristl, Effect of resveratrol incorporated in liposomes on proliferation and UV-B protection of cells, Int. J. Pharm. 363 (2008) 183–191, http://dx.doi.org/10.1016/j.ijpharm.2008.07.024.

[13] C. Caddeo, O. Díez-Sales, R. Pons, X. Fernàndez-Busquets, A. Fadda, M. Manconi, Topical anti-inflammatory potential of quercetin in lipid-based nanosystems: in vivo and in vitro evaluation, Pharm. Res. 31 (2014) 959–968, http://dx.doi.org/10.1007/s11095-013-1215-0.

[14] D. Paolino, D. Cosco, F. Cilurzo, E. Trapasso, V.M. Morittu, C. Celia, et al., Improved in vitro and in vivo collagen biosynthesis by asiaticoside-loaded ultradeformable vesicles, J. Control Release 162 (2012) 143–151, http://dx.doi.org/10.1016/j.jconrel.2012.05.050.

[15] M.L. Manca, M. Manconi, A.M. Falchi, I. Castangia, D. Valenti, S. Lampis, et al., Close-packed vesicles for diclofenac skin delivery and fibroblast targeting, Colloids Surf. B Biointerfaces 111 (2013) 609–617, http://dx.doi.org/10.1016/j.colsurfb.2013.07.014.

[16] M.L. Manca, M. Zaru, M. Manconi, F. Lai, D. Valenti, C. Sinico, et al., Glycerosomes: a new tool for effective dermal and transdermal drug delivery, Int. J. Pharm. 455 (2013) 66–74, http://dx.doi.org/10.1016/j.ijpharm.2013.07.060.

[17] I. Castangia, A. Nácher, C. Caddeo, D. Valenti, A.M. Fadda, O. Díez-Sales, et al., Fabrication of quercetin and curcumin bionanovesicles for the prevention and rapid regeneration of full-thickness skin defects on mice, Acta Biomater. 10 (2014) 1292–1300, http://dx.doi.org/10.1016/j.actbio.2013.11.005.

[18] M. Gupta, U. Agrawal, S.P. Vyas, Nanocarrier-based topical drug delivery for the treatment of skin diseases, Expert Opin. Drug Deliv. 9 (2012) 783–804, http://dx.doi.org/10.1517/17425247.2012.686490.

[19] M. Takahashi, D. Kitamoto, Y. Asikin, K. Takara, K. Wada, Liposomes encapsulating Aloe vera leaf gel extract significantly enhance proliferation and collagen synthesis in human skin cell lines, J. Oleo Sci. 58 (2009) 643–650. http://www.ncbi.nlm.nih.gov/pubmed/19915322 (accessed 04.09.14.).

[20] A. Munin, F. Edwards-Lévy, Encapsulation of natural polyphenolic compounds; a review, Pharmaceutics 3 (2011) 793–829, http://dx.doi.org/10.3390/pharmaceutics3040793.

[21] S. Pinsuwan, T. Amnuaikit, S. Ungphaiboon, A. Itharat, Liposome-containing *Hibiscus sabdariffa* calyx extract formulations with increased antioxidant activity, improved dermal penetration and reduced dermal toxicity, J. Med. Assoc. Thail. 93 (Suppl. 7) (2010) S216–S226. http://www.ncbi.nlm.nih.gov/pubmed/21294418 (accessed 04.09.14.).

[22] J.C.M. Stewart, Colorimetric determination of phospholipids with ammonium ferrothiocyanate, Anal. Biochem. 104 (1980) 10–14, http://dx.doi.org/10.1016/0003-2697(80)90269-9.

[23] G. Pabst, M. Rappolt, H. Amenitsch, P. Laggner, Structural information from multilamellar liposomes at full hydration: full q-range fitting with high quality x-ray data, Phys. Rev. E 62 (2000) 4000–4009. http://link.aps.org/doi/10.1103/PhysRevE.62.4000.

[24] C. Caddeo, M. Manconi, A.M. Fadda, F. Lai, S. Lampis, O.D. Sales, et al., Nanocarriers for antioxidant resveratrol: formulation approach, vesicle self-assembly and stability evaluation, Colloids Surf. B Biointerfaces 111 (2013) 327–332, http://dx.doi.org/10.1016/j.colsurfb.2013.06.016.

[25] S.O. Oyedemi, A.J. Afolayan, Antibacterial and antioxidant activities of hydroalcoholic stem bark extract of Schotia latifolia Jacq, Asian Pac. J. Trop. Med. 4 (2011) 952–958, http://dx.doi.org/10.1016/S1995-7645(11)60225-3.

[26] T.C.P. Dinis, V.M.C. Madeira, L.M. Almeida, Action of phenolic derivatives (Acetaminophen, Salicylate, and 5-Aminosalicylate) as inhibitors of membrane lipid peroxidation and as peroxyl radical scavengers, Arch. Biochem. Biophys. 315 (1994) 161–169, http://dx.doi.org/10.1006/abbi.1994.1485.

[27] C. Caddeo, O.D. Sales, D. Valenti, A.R. Saurí, A.M. Fadda, M. Manconi, Inhibition of skin inflammation in mice by diclofenac in vesicular carriers: liposomes, ethosomes and PEVs, Int. J. Pharm. 443 (2013) 128–136, http://dx.doi.org/10.1016/j.ijpharm.2012.12.041.

[28] L. Löbbecke, G. Cevc, Effects of short-chain alcohols on the phase behavior and interdigitation of phosphatidylcholine bilayer membranes, Biochim. Biophys. Acta Biomembr. 1237 (1995) 59–69, http://dx.doi.org/10.1016/0005-2736(95)00076-F.

[29] T.-T. Phan, P. See, S.-T. Lee, S.-Y. Chan, Protective effects of curcumin against oxidative damage on skin cells in vitro: its implication for wound healing, J. Trauma Inj. Infect. Crit. Care 51 (2001) 927–931.

[30] C. Caddeo, M. Manconi, A.M. Fadda, F. Lai, S. Lampis, O. Diez-Sales, et al., Nanocarriers for antioxidant resveratrol: formulation approach, vesicle self-assembly and stability evaluation, Colloids Surf. B Biointerfaces 111C (2013) 327–332, http://dx.doi.org/10.1016/j.colsurfb.2013.06.016.

[31] Z. Abramovic, U. Sustarsic, K. Teskac, M. Sentjurc, J. Kristl, Influence of nanosized delivery systems with benzyl nicotinate and penetration enhancers on skin oxygenation, Int. J. Pharm. 359 (2008) 220–227, http://dx.doi.org/10.1016/j.ijpharm.2008.03.014.

[32] V. Torchilin, Fluorescence microscopy to follow the targeting of liposomes and micelles to cells and their intracellular fate, Adv. Drug Deliv. Rev. 57 (2005) 95–109, http://dx.doi.org/10.1016/j.addr.2004.06.002.

[33] R. Angelico, A. Ceglie, P. Sacco, G. Colafemmina, M. Ripoli, A. Mangia, Phytoliposomes as nanoshuttles for water-insoluble silybin-phospholipid complex, Int. J. Pharm. 471 (2014) 173–181, http://dx.doi.org/10.1016/j.ijpharm.2014.05.026.